DSTO-TR-0224

DSTO

Computational Fluid Dynamics Modelling of the Australian Challenge

G. Kemister

DEPARTMENT OF DEFENCE

DEFENCE SCIENCE AND TECHNOLOGY ORGANISATION

DISCLAIMER NOTICE

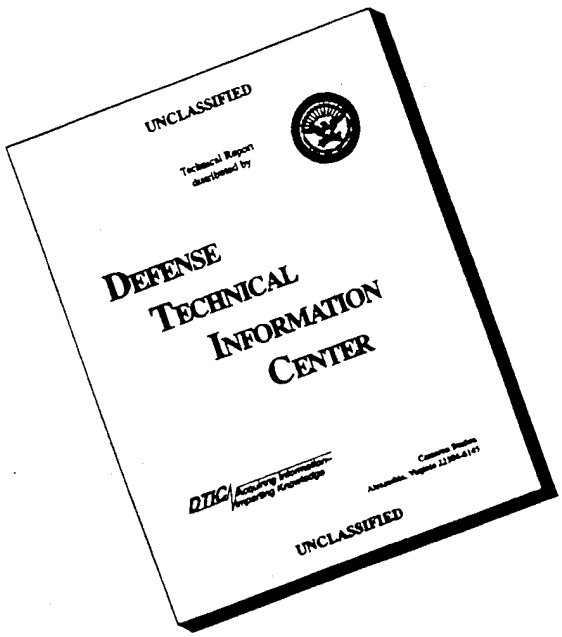

THIS DOCUMENT IS BEST QUALITY AVAILABLE. THE COPY FURNISHED TO DTIC CONTAINED A SIGNIFICANT NUMBER OF PAGES WHICH DO NOT REPRODUCE LEGIBLY.

Computational Fluid Dynamics Modelling of the Australian Challenge

G. Kemister

Weapons Systems Division
Aeronautical and Maritime Research Laboratory

DSTO-TR-0224

ABSTRACT

The Australian Challenge was a set of experiments chosen as a test case to establish how well computer calculations can model the blast overpressure around a complex set of structures. This paper presents the first three dimensional calculation on the Australian Challenge using CFD codes. These codes have been developed at AMRL and the Australian Challenge represents their first test in a 'real world' scenario. The calculations show good agreement with the experimental results. The program can now be used with a good degree of confidence in modelling other complex scenarios, reducing the need for expensive experimentation. The safety aspects of any changes in operational procedure can be evaluated quickly and efficiently.

DEPARTMENT OF DEFENCE

DEFENCE SCIENCE AND TECHNOLOGY ORGANISATION

Published by

DSTO Aeronautical and Maritime Research Laboratory
PO Box 4331
Melbourne Victoria 3001 Australia

Telephone: (03) 9626 7000
Fax: (03) 9626 7999

AR No. 009-356
September 1995

APPROVED FOR PUBLIC RELEASE

Computational Fluid Dynamics Modelling of the Australian Challenge

EXECUTIVE SUMMARY

The 1994 Australian white paper on Defence "Defending Australia" requires that the Australian Defence Forces be ready to defend against a short warning conflict. A short warning conflict could vary between a series of low level raids to a larger, more protracted operation. In these scenarios it is very conceivable that the forces would require rapid entry into structures, usually buildings, to achieve their mission. The obvious way to do this is through an explosive charge either on a wall, door or window. The question then becomes what is the distance to stand away from the explosive charge to prevent any injuries and also what is the likely effect on the people inside the building. This can be answered by performing an expensive series of experimental trials or by using a reliable computer simulation. This paper presents numerical simulation for a specific set of scenarios for which experimental results are available as a way of validating the computer program in a realistic complex situation.

The scenarios modelled were issued as a challenge to the numerical modellers within the TTCP nations. This paper presents the first results for these scenarios based on computational fluid dynamics (CFD) using full three-dimensional geometry. The scenarios consist of explosive charges detonating on a concrete reinforced wall of a building which may or may not have open windows and doors. The blast overpressure from the explosion was calculated and compared against the experimental results in considerable detail. This allowed for an analysis of the approximations used within the calculations and an estimate of their impact on the computed results.

The computational results show that the program has the ability to successfully calculate the blast overpressure from an explosion in a structurally complex scenario. This validation of the program will allow it to be used with confidence to model complex operational scenarios requiring the rapid entry of forces into buildings. It will reduce dramatically the need for expensive and time-consuming trials in this area and allow hypothetical situations to be explored. It will also allow the safety of current operational procedures to be evaluated, as well as any proposed changes to these procedures.

Author

G. Kemister

Weapons Systems Division

Gary Kemister graduated from Sydney University in 1980 with a B.Sc (Hons I) and in 1985 with a Ph.D. in theoretical chemistry. After working at Oxford University, University of North Carolina at Chapel Hill, Sydney University and La Trobe University on various aspects of electronic structure of materials he joined the Defence Department in 1991 working for the Analytical Studies Unit in Force Development and Analysis Division in Canberra. In 1993 he moved to Explosive Ordnance Division (now part of Weapons Systems Division) at Maribyrnong and is currently working on numerical simulations of the physics and chemistry of explosions.

Contents

1. Introduction

The 1994 Australian white paper on Defence "Defending Australia" requires that the Australian Defence Forces be ready to defend against a short warning conflict. A short warning conflict could vary between a series of low level raids to a larger, more protracted operation. In these scenarios it is very conceivable that the forces would require rapid entry into structures, usually buildings, to achieve their mission. The obvious way to do this is through an explosive charge either on a wall, door or window. The question then becomes what is the distance to stand away from the explosive charge to prevent any injuries and also what is the likely effect on the people inside the building. To answer these questions experimental trials have been conducted in selected scenarios and the overpressures measured. However experimental trials are expensive and specific to the selected scenario, consequently it is better to be able to model scenarios and their variations with a computer simulation which has been validated against experimental measurements. This work is the validation of the computer model developed at WSD AMRL against a set of experimental overpressure measurements in a complex building scenario.

The Australian Challenge consists of two sets of air blast data recorded by AMRL in 1990 at Woomera, South Australia, as part of the collaborative demolition trials conducted under the auspices of The Technical Cooperation Program (TTCP) [1]. The test series from which the results were generated comprised a number of firings of experimental contact breaching charges against the walls of derelict reinforced concrete buildings. Air blast gauges were positioned around the building returns to assess the feasibility of personnel firing the charges in close proximity, but out of line of sight. The air blast results have been circulated around the TTCP nations as a test for the modelling capability of blast overpressure calculations. Several attempts [2,3,4] have been made to model these experimental results with generally good agreement, however the previous calculations have been limited by approximations concerning the geometry of the experimental set-up. In the calculations reported here we have modelled the buildings in full 3-D representation and compared the results to both the experimental and previous computational results.

2. Experimental Details

The Australian Challenge consists of sets of experimental results for two selected building layouts. The layout for the first experiment, event number three, is shown in Figure 1 and the layout for the second experiment, event number ten, is shown in Figure 2. Note that event 3 and event 10 were conducted at opposite ends of the building structures. Photographs of the buildings showing damage sustained prior to the conduct of the tests being analysed in this paper are shown in Figure 3. These photographs are taken from the end of the buildings where event 3 was conducted.

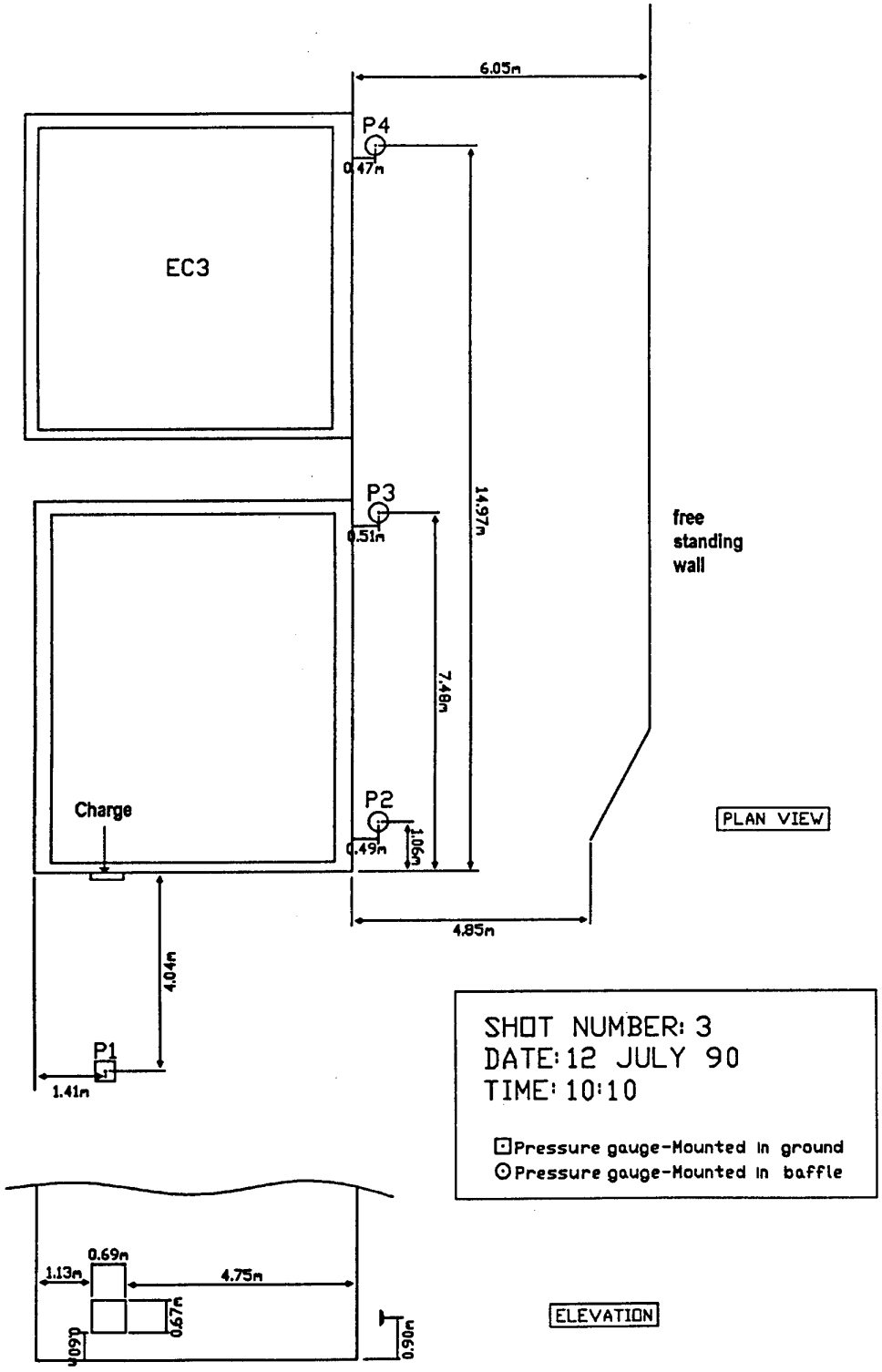

Figure 1. Experimental layout for event number three.

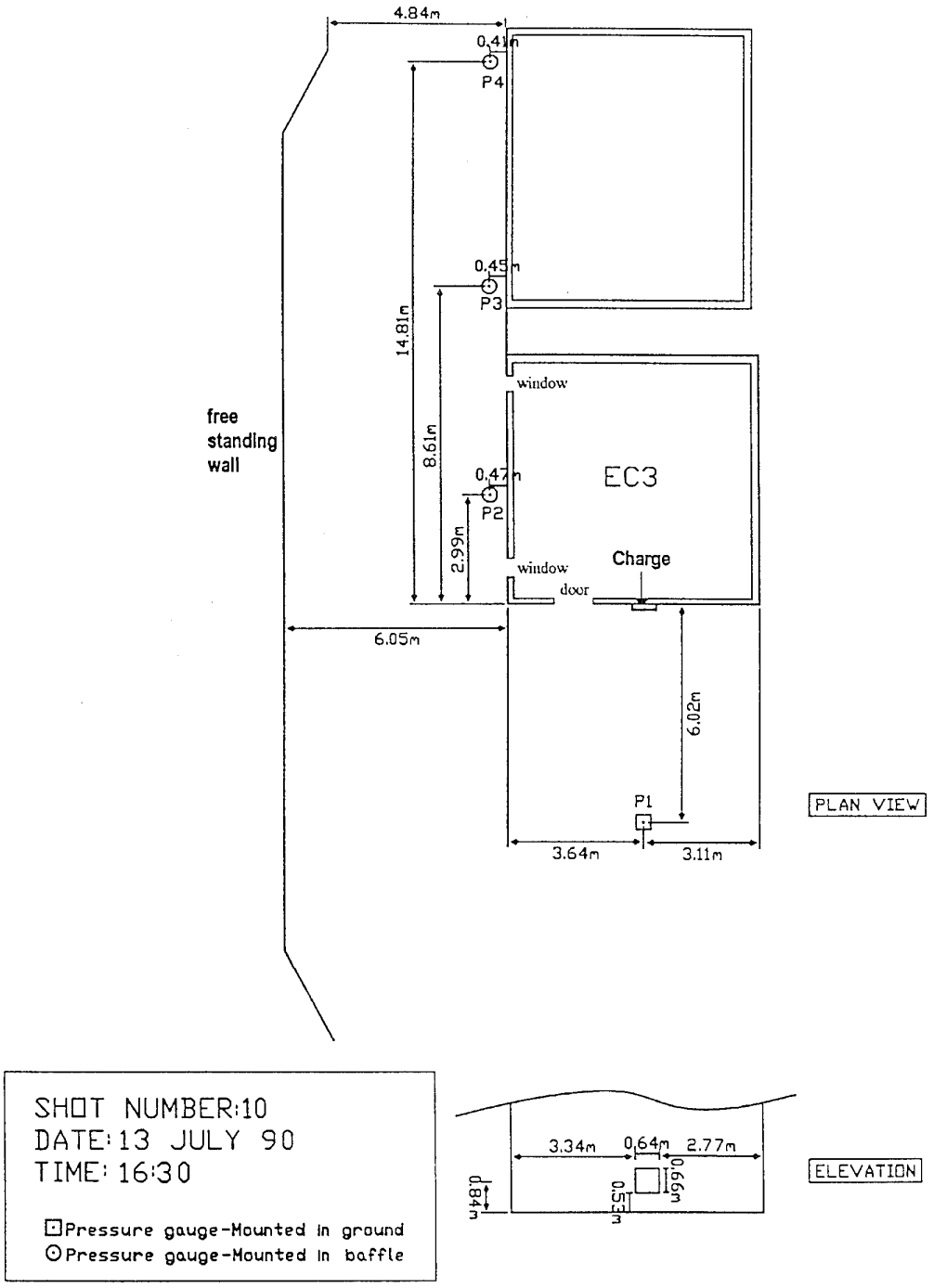

Figure 2. Experimental layout for event number ten.

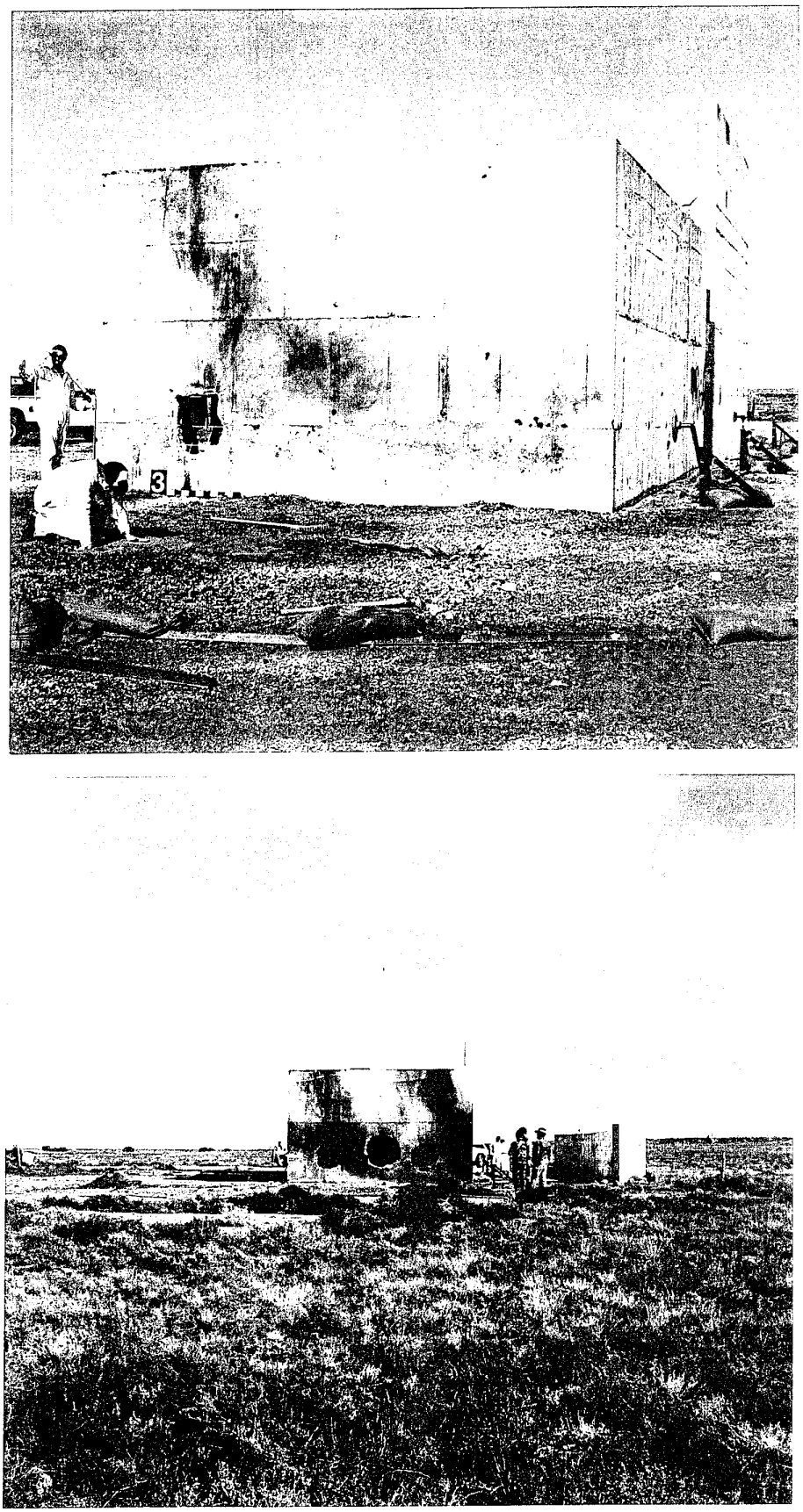

Figure 3. Photographs of the buildings.

In each experiment a charge was detonated to breach the wall of the building and blast overpressure measurements were recorded at four locations outside the building. The breaching charges, in each case, consisted of four copper lined linear shaped charges, each 500mm in length, arranged in a square array. Plastic Explosive No. 4 (88% RDX, 11% grease and 1% PEDO) was used to fill the charges which were initiated simultaneously with detonating cord (Fig 4).

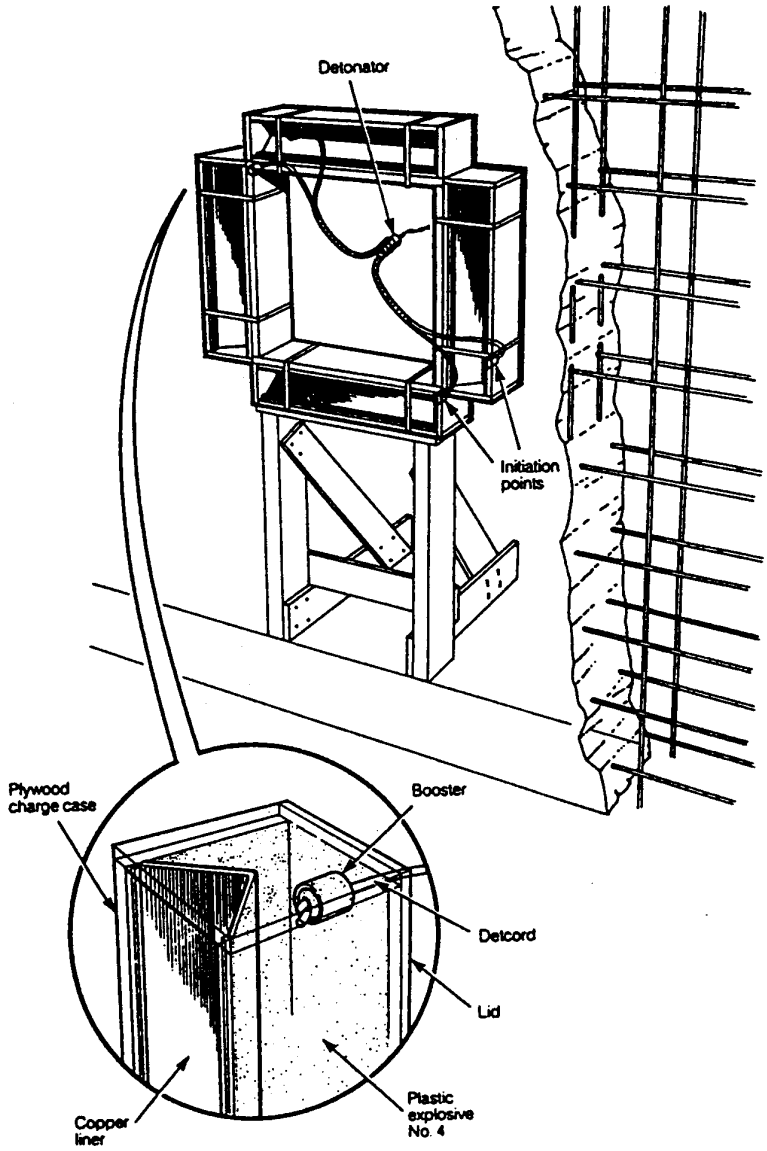

Figure 4. Sketch of demolition charge.

Event 3 - For event 3 the charge weight was 8.72 kg. Event 3 is characterised by a free standing wall (1.8m high) with a bend in it around the corner from where the charge is detonated (see Figure 1).

Event 10 - For event 10 the charge weight was 21.6 kg. In event 10 the building is characterised by two holes caused by previous events which for our purposes will be considered as windows and a door. There is also a free standing wall (1.8m high) parallel to the structure (see Figure 2).

Pressure gauges were placed at the positions P1, P2, P3 and P4 marked on Figures 1 and 2. The experimental time-pressure traces were recorded for each gauge and each event at several sampling speeds, for example, the time-pressure trace for gauge 1 in event 3 was recorded at time intervals of 8 ns, 40 ns and 160 ns with each being recorded for 512 steps. Thus the recordings span different time lengths, being 4.096 ms, 20.48 ms and 81.92 ms respectively. All of the experimental traces used in this paper are for the longest time step i.e., 160 ns, extending out to ~80 ms. These traces were chosen because they most closely correspond to the time step used in the calculations. The time step is initially 80 ns but increases in length as the speed of the pressure front decreases. Variable time steps were used to improve the efficiency of the calculation as they can cut the number of time steps required to reach a particular time point by approximately one-third. For example the time step is about 320 ns by the time the calculation has finished.

Further experimental details can be obtained from Reference 1.

3. Computational Details

The calculations were performed using a 3-dimensional finite difference computer program, developed at AMRL [5], which solves the Euler equations for the conservation of mass, momentum and energy of an inviscid, compressible fluid (in this case air). A 3-dimensional Cartesian grid with fixed spacing was used as a basis for the calculation. Operator splitting, which reduces the complexity of a 3-dimensional calculation down to three 1-dimensional calculations at each time-step and grid point, was also used. A 1-dimensional Flux-Corrected Transport (FCT) algorithm, with fourth order phase accuracy and an overall second order accuracy on uniform grids, was used to solve the 1-dimensional calculations [6]. Rigid wall boundary conditions were used for the walls and the ground in the calculations whilst outflow boundary conditions were used at all the other edges of the computational grid. The computational cell size was $\delta x = \delta y = \delta z = 20$ cm and the largest grid size used was 95 x 130 x 60 giving 741,000 cells. The time step was calculated at each iteration. In order to perform the calculations without reprogramming the code each time to take into account different geometries, modifications were made to the code to allow the input of an arbitrary shape (within the restriction of the fixed Cartesian grid) and these modifications are described in more detail in Appendix 1. The calculations were performed on either the EOD(S) RISC computer (eodrisc-6000s.dsto.gov.au) or the EOD(M) HP workstation (eod-hp1.dsto.gov.au).

To begin the calculations requires the simulation of an explosion on the wall. This can be modelled using the full chemistry and physics of the explosion; however this is both difficult and time-consuming in a calculation of this size. Furthermore it contains a large amount of detailed information close in to the explosion that is simply washed out by the time the pressure pulses reach any of the pressure gauges. Combustion Dynamics [3] have developed an approximate method of starting calculations without modelling the full explosion which gives the correct behaviour in the far-field, i.e., a sufficient distance away from the explosion. In this approximation 1kg of TNT (or equivalent) is replaced by 0.0164 m^3 of gas at a pressure of 1000 atmospheres and a temperature of 3000K. Thus, for example in event 3, 8.72 kg of PE4 with a TNT equivalence of 1.35 gives an equivalent weight of TNT of 11.772 kg and a volume of 0.193 m^3. The gas bubble approximation has been used in all the calculations reported here.

The gas bubble approximation to an explosive is designed to give the correct energy content for the explosive. In the far-field this will give the correct time-pressure trace to within the computational accuracy. However, in the near field it will be unable to accurately represent the sharp peak caused by the explosive because of the assumption of an equal pressure everywhere inside the gas bubble and because of the finite size of the grid. The finite grid size can be overcome by making it sufficiently small however this can result in the calculation either being too large to fit in the memory of the available workstations or requiring an inordinate length of time to perform the calculations. Another factor affecting accuracy in the near field is the shape of the explosive. The explosive has a much smaller volume than the gas bubble and therefore any fine details of the explosive shape may be lost when it is replaced by the larger gas bubble volume which in itself is restricted to cells defined by the grid. Whether these details are important depends on the distance at which the interactions with the structures occur and at which the measurements are taken.

The four linear shaped charges used in the experiments were arranged in a square array as shown in Fig 4. Given the grid size that is needed to make the full computation feasible within a reasonable length of time (i.e., 20 cm cell size), the explosive is approximated by a volume of gas 1 cell deep (20cm) by 2 cells wide (40 cm) by the length required to make the correct volume of the equivalent explosive weight, diagrammatically shown in Figure 5. The size of the square is enlarged to avoid any problems caused by overlapping squares and to maintain the correct relative geometry. This is a coarse approximation in close but it is reasonable in the far-field. One way of improving this approximation is to break the calculation up into separate problems, that is, near field measurements and far-field measurements, where a much finer grid is used to calculate the near field measurements (e.g., 2 cm). This will allow more cells in which to resolve the peak pressure in the near field at the expense of doing an extra calculation.

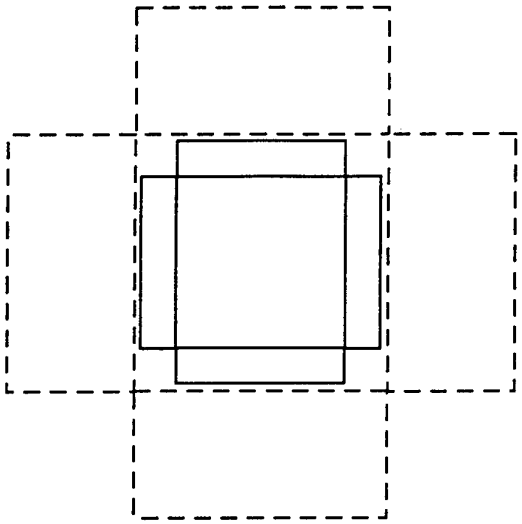

Figure 5. Diagrammatic sketch of the explosive setup. The solid lines are the explosive and the dashed lines are the 'gas bubble' approximation.

4. Results

Combustion Dynamics have modelled the Australian Challenge in a two dimensional axisymmetric grid [3]. In this approximation the axis of symmetry is through the centre of the charge on the wall and everything is then radially symmetric about that axis. Thus the free standing wall is modelled as a cylinder with a radius of approximately 10m from the charge. Their results show good agreement for the first peak reaching the pressure gauge but the subsequent peaks are modelled less accurately due to the inability to model the 1.8 m wall correctly in the cylindrical coordinates.

Jones [2] has modelled event 3 of the Australian Challenge in a similar way to this work but only looking at the first 3 gauges due to computational constraints. The program used in this paper is a development of the Jones program.

There was no time of arrival data available from the experiments and so, for comparison purposes, the initial arrival of the experimental curve and the computational curve have been superimposed. This allows for analysis of the relative time of arrival of the various peaks.

Event 3.

The experimental results (solid line) and the results of our calculations (dashed line) for pressure gauges 1 to 4 in Event 3 are given in Figures 6, 8, 9, and 12 respectively. The peak pressures for this event are tabulated in Table 1.

Table 1. Peak experimental and calculational pressures for gauges 1 to 4 in Event 3.

Gauge Number	Peak Overpressure (kPa) Experiment	Peak Overpressure (kPa) Simulation
1	1130	636
2	47	42
3	11.7	15
4	5.0	10

It can be seen from Figure 6 and especially Table 1 that the peak pressure given by the computations at gauge 1 is significantly lower than the experimentally recorded peak pressure. The single pressure pulse with little other structure seen in Figure 6 is the expected result for a pressure gauge at this distance from this size explosion. The small pulse in the calculation at ~ 20 ms is the secondary expansion of the explosive. The experimental pulse for the secondary expansion is not obvious in Figure 6, presumably being swamped by the large effects of the main peak.

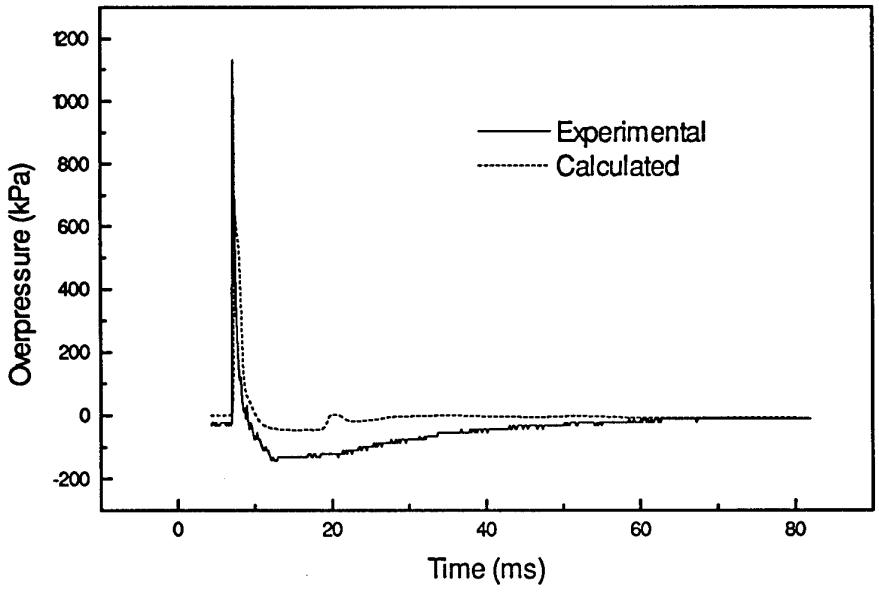

Figure 6. Plot of Overpressure versus Time for Gauge 1 in Event 3.

The lower peak pressure given by the calculation is due to the coarse grid size (20 cm cells) used in the full calculation. By repeating the calculation with a grid size of 4 cm and a correspondingly smaller timestep, but only looking at gauge 1, (it is impractical due to the size of the grid to include any other gauge positions), the effect of the cell size on the calculation can be inferred. The pressure plot for this calculation is given in Figure 7.

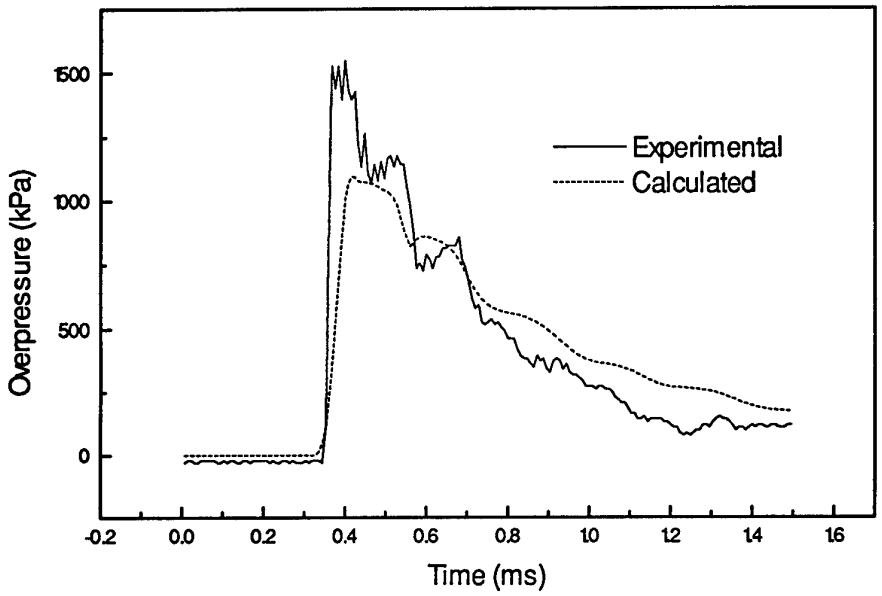

Figure 7. Plot of Overpressure vs Time for Gauge 1 in Event 3 using a finer computational grid size and timestep and comparing it against a finer time recording of the experimental results.

The experimental peak pressure in Figure 7 is 1550 kPa and is higher than the value quoted in Table 1 (1130 kPa) since the experimental sampling rate is higher in this reading. That is, for this comparison, the calculations are being compared with the experimental results which were taken at 8ns time intervals rather than the 160 ns used for the comparisons in the rest of this paper. For this section of the work the calculations were performed with a timestep in the range 4 - 32 ns, varying with the speed of the pressure front (as for the other calculations in this paper). The peak pressure for the calculation in Figure 7 is 1100 kPa (compared to the value of 636 kPa given in Table 1).

Figure 7 also shows that the calculation does not resolve the sharpness of the initial rise in pressure to match the experiment. This is directly related to the cell size and timestep in the calculation. The calculation can not hope to resolve a rise time of the order of 1 ns if the timestep is of the order of 4 ns, thus the pressure curve from the calculation in Figure 7 has a much more rounded shape than the experimental curve. Apart from the resolution of the initial peak there is good agreement between the experimental and computational curves.

The pressure trace given in Figure 8 and the peak pressures given in Table 1 for gauge 2 show quite good agreement between the experiment and the calculation. As the gauge is just around the corner there is no discernible reflection from the adjacent concrete wall. There is a possibility of a peak at about 18 ms in the experimental trace which could be identified as the secondary expansion of the explosion. The secondary expansion in the computation is significantly delayed due to the gas bubble approximation and occurs at ~ 22 ms.

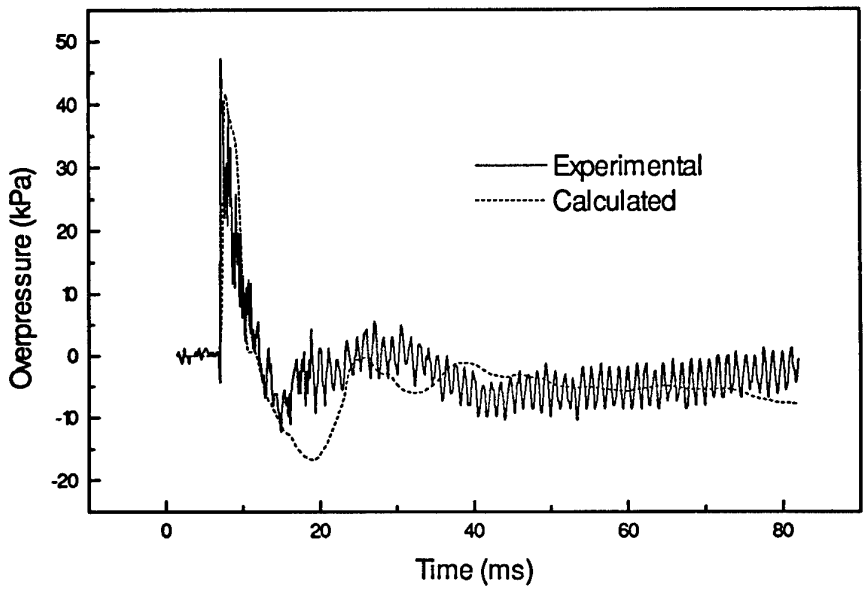

Figure 8. Plot of Overpressure versus Time for Gauge 2 in Event 3.

The pressure trace given in Figure 9 and the peak pressures given in Table 1 for gauge 3 show reasonable agreement between the experiment and the calculation. The peak pressure for the calculation overestimates the experimental peak pressure but only by ~3 kPa. The most noticeable difference between the experimental and computational pressure traces is the pressure peak in the experimental trace at about 23 ms compared with a dip in the computational trace at that time. Given the time delay between the initial peak and this peak, about 15 ms, this peak is consistent with a reflection off the angled end of the adjacent concrete wall. The absence of this peak in the calculation is probably due to the approximate representation of this section of the concrete wall (see Figure 10). Since the calculation sees this angled piece of wall in a step-wise manner, the reflection off this piece of wall must be lost due to the coarseness of the representation.

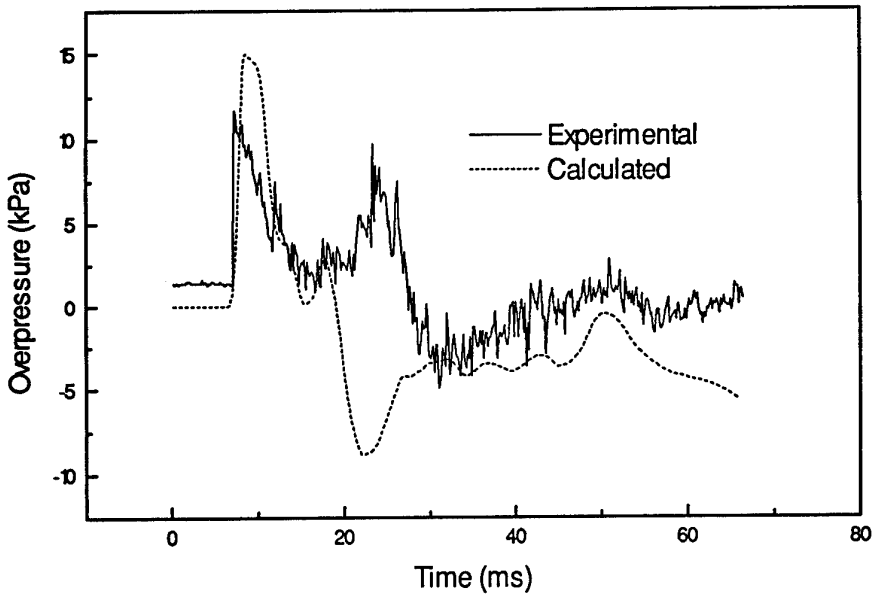

Figure 9. Plot of Overpressure versus Time for Gauge 3 in Event 3.

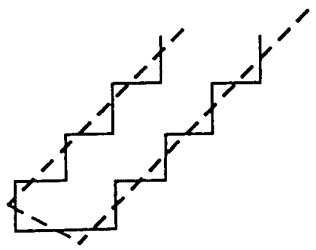

Figure 10. Angled wall (dashed line) and its stepwise representation in the computation (solid line).

A further possibility for the inability to model the experimental reflected pressure peak correctly could be the orientation of the pressure gauge. The experimental pressure gauge was mounted in a baffle plate which was positioned such that the sensing surface of the gauge faced and was parallel to the wall. This results in clean traces when the shock wave is travelling across the baffle plate (ie, side on or incident pressure) but acts as a reflecting surface when the shock wave is travelling towards the baffle plate. In this case, the shock wave which has diffracted around the corner of the building, travels across the baffle plate resulting in a clean trace. However, the shock wave which has reflected off the retaining wall and then off the wall of the building travels towards the baffle plate, resulting in higher pressures due to the interaction with the baffle plate. This is represented schematically in figure 11.

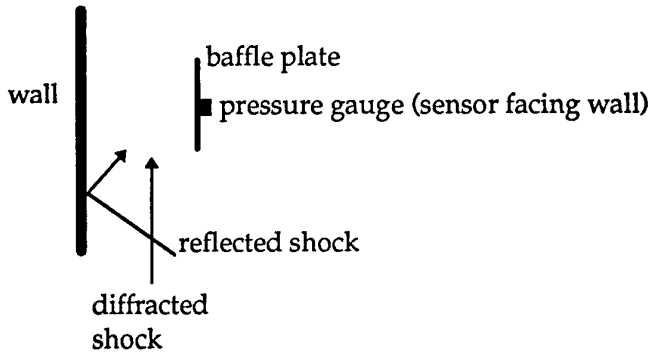

Figure 11. Diagram of setup of pressure gauges 2, 3 and 4

The pressure trace given in Figure 12 and the peak pressures given in Table 1 for gauge 4 show qualitative agreement between the experiment and the calculation. The peak pressure is overestimated but is well within expectations. The reflection from the concrete retaining wall (at about 20 ms) shows good time agreement but the magnitude is substantially underestimated. This is probably due to the reasons discussed for gauge 3. The experimental trace is also complicated by a "ringing", due to the baffle plate oscillating at a particular frequency.

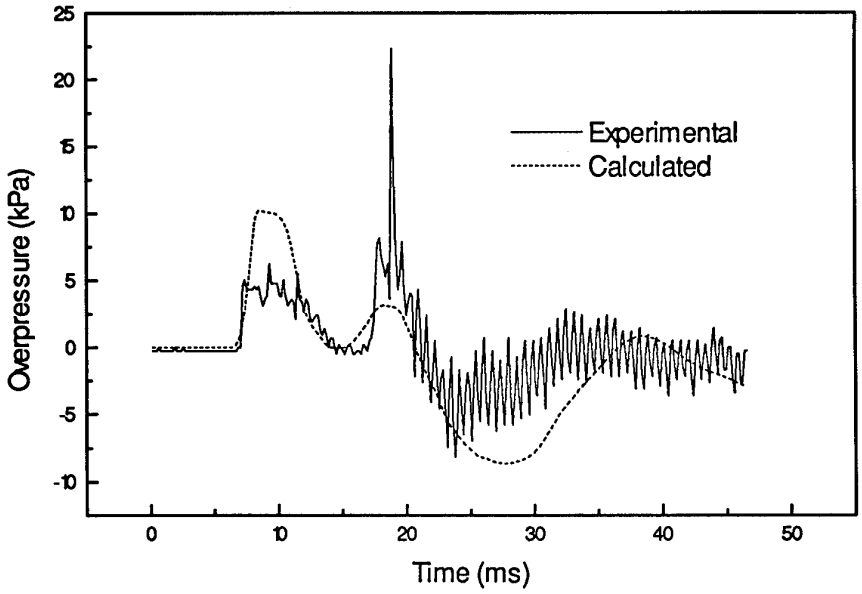

Figure 12. Plot of Overpressure versus Time for Gauge 4 in Event 3.

Figures 13a - 13h show pressure contour plots for Event 3 at a height of 0.9 m above the ground, i.e., at the height of the midpoint of the explosive and the pressure gauges. Figure 13a has an approximate outline of the buildings and the wall superimposed on the plot to give an idea of their location. Unfortunately the structures are not added onto the contour plots when they are drawn. The contour plots show the initial shock expanding out from the explosion site (13b), diffracting around the corners of the building (13c,13d) and reflecting off the concrete retaining wall (13e,13f,13g). The contour plots provide a clearer understanding of what is happening during the course of the movement of the shock front.

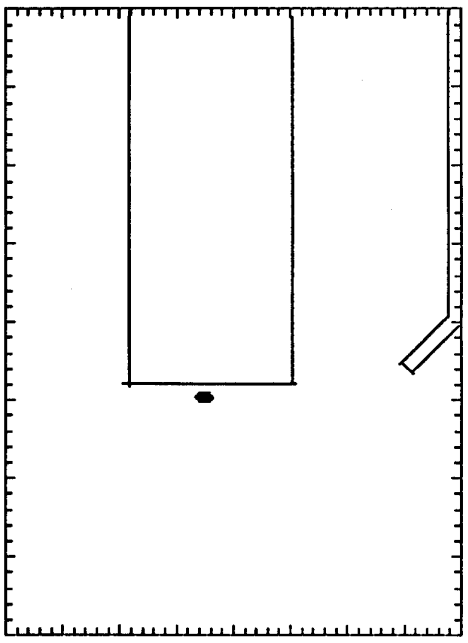

Figure 13a. 0ms contours with building outline superimposed

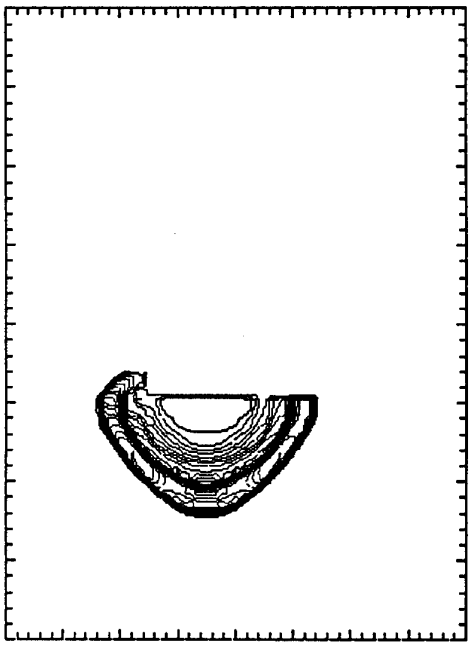

Figure 13b 3.5ms contours

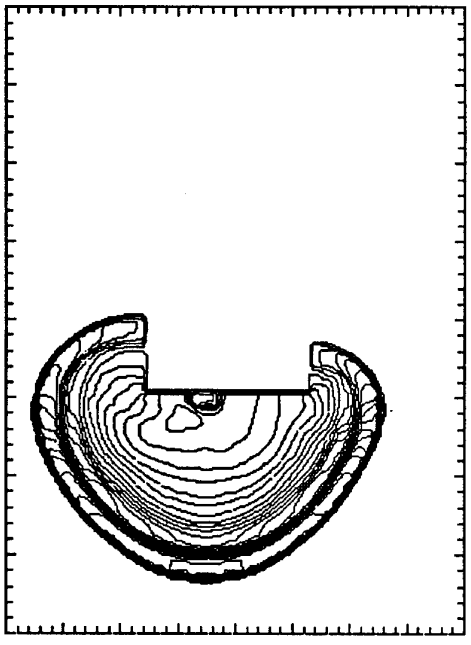

Figure 13c 7.9ms contours

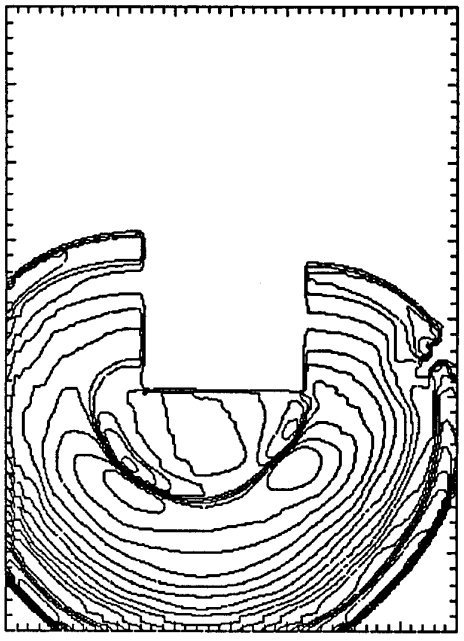

Figure 13d 14.2ms contours

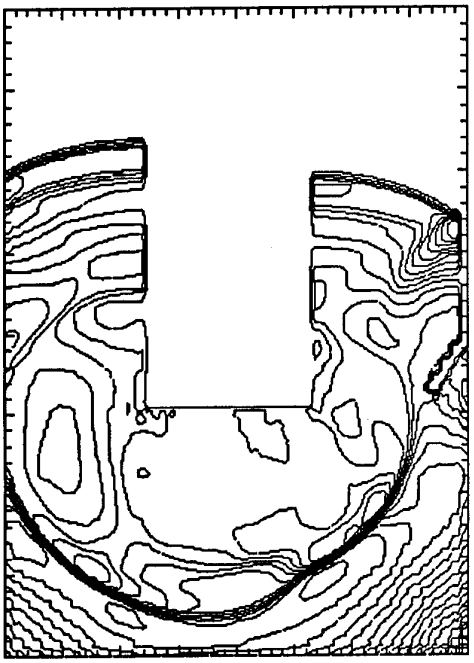

Figure 13e 26.9ms contours

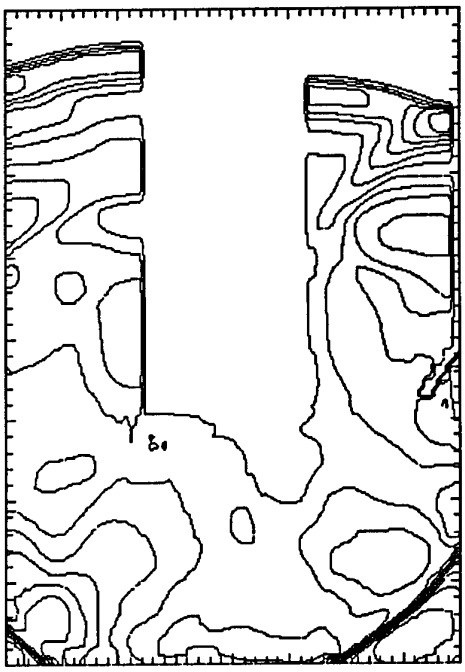

Figure 13f 37.2ms contours

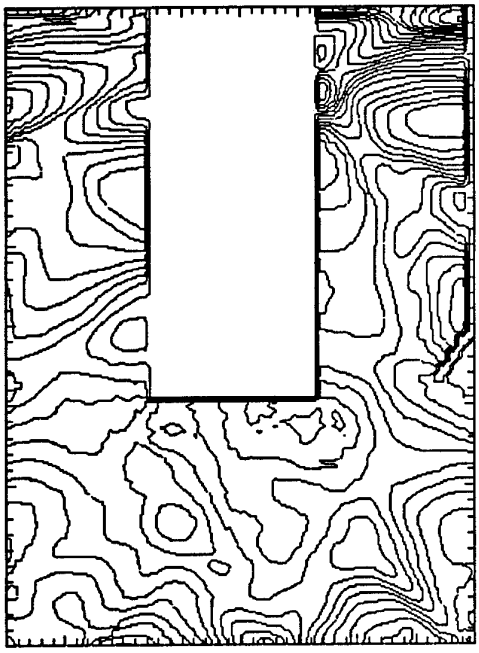

Figure 13g 48.1ms contours

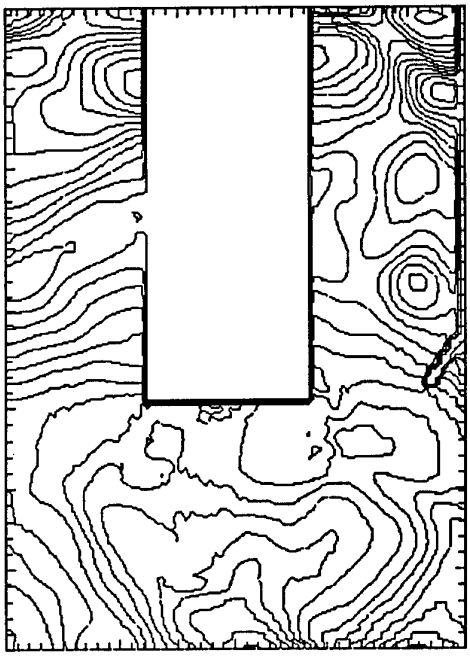

Figure 13h 59.3ms contours

Event 10.

The experimental results (solid line) and the results of our calculations (dashed line) for pressure gauges 1 to 4 in Event 10 are given in Figures 14 to 17 respectively. The peak pressures for this event are tabulated in Table 2. Note that the calculations were done with a reflection through the axis of the buildings for computational simplicity.

Table 2. Peak experimental and calculational pressures for gauges 1 to 4 in Event 10.

Gauge Number	Peak Overpressure (kPa) Experiment	Peak Overpressure (kPa) Simulation
1	780	700
2	62	47
3	33.6	23.6
4	15.9	14.9

It can be seen from the plot of the pressure-time traces in Figure 14 and the peak pressure values given in Table 2 that, for gauge 1 in Event 10, there is much closer agreement than was the case for Event 3. This is due to the fact that the pressure gauge was further away from the explosion (6 m as compared to 4 m in Event 3) and consequently the shock front has longer (i.e., more computational cells) to resolve itself.

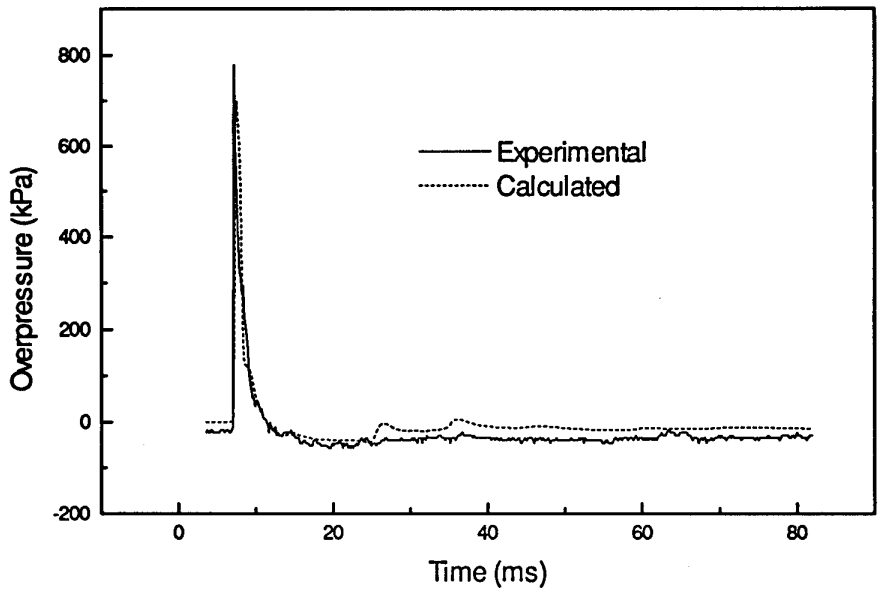

Figure 14. Plot of Overpressure versus Time for Gauge 1 in Event 10.

The pressure traces for gauge 2 in Event 10 are given in Figure 15 and the peak pressures are given in Table 2. These pressure traces are in good agreement, with the only difference being attributable to the secondary expansion of the explosion (at 18 ms in the experimental trace and probably part of the peak at about 30 ms in the computation).

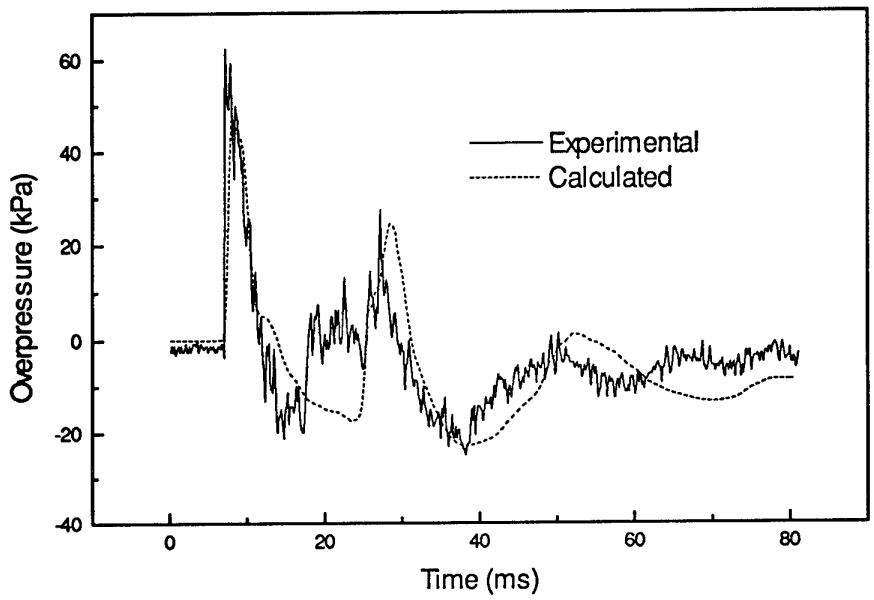

Figure 15. Plot of Overpressure versus Time for Gauge 2 in Event 10.

The pressure traces for gauge 3 in Event 10 are given in Figure 16 and the peak pressures are given in Table 2. The traces show good overall qualitative agreement, however certain fine features show a marked difference. There is a small pressure spike before the main diffracted shock reaches the gauge. This spike, which was present in the Combustion Dynamics 2D cylindrical calculation[3], was identified as the shock wave travelling through the room in the building and arriving at the gauge before the shock front which diffracted around the building. This was not evident in the current calculations and is likely due to the inclusion of the blast hole caused by the explosive in the Combustion Dynamics calculation. In the present calculation it was assumed that the structural response of the building, i.e., the creation of the blast hole, occurred on a much longer timescale than the initial shock wave travelling around the building.

The reflection of the shock wave off the retaining wall arrives at approximately the same time in the experimental and computational traces (~22 ms) but is much stronger in the experimental case. This difference is attributed to the orientation of the baffle plate on the pressure gauge (see the discussion on gauge 3 in Event 3). In the

calculated pressure trace there is also a large peak at about 50 ms which is not evident in the experimental pressure trace. The contours in Figures 18g and 18h give some evidence that this is caused by the second reflection of the shock wave off the retaining wall combining with the first reflection of the secondary expansion off the retaining wall. In the calculation the secondary occurs later than in the experiment due to the gas bubble approximation. Thus in the experiment these multiply reflected shock waves show up as separate shocks with considerably smaller magnitudes.

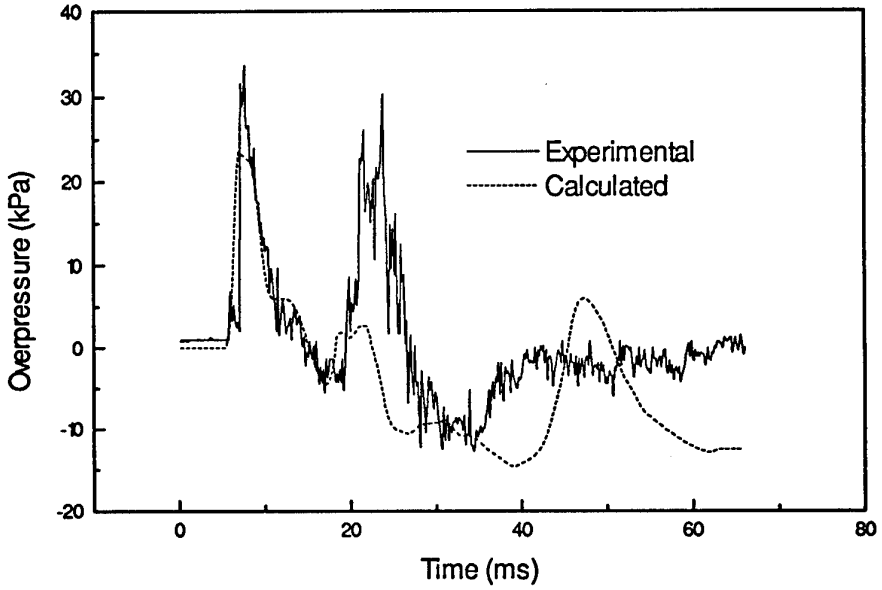

Figure 16. Plot of Overpressure versus Time for Gauge 3 in Event 10.

The pressure traces for gauge 4 in Event 10 are given in Figure 17 and the peak pressures are given in Table 2. The initial diffracted peak in the experimental trace shows good agreement with the calculated diffracted peak. The first reflected peak (about 20 ms) in the calculation just precedes the experimental peak in time but the size of the peak is in reasonable agreement. The next peak in the experimental trace (about 35 ms) is missing from the computation due to the omission of the angled section of the concrete retaining wall near gauge 4 as a simplifying measure (see Figure 2 for the experimental layout). There is good agreement with the next reflected peak at about 45 ms.

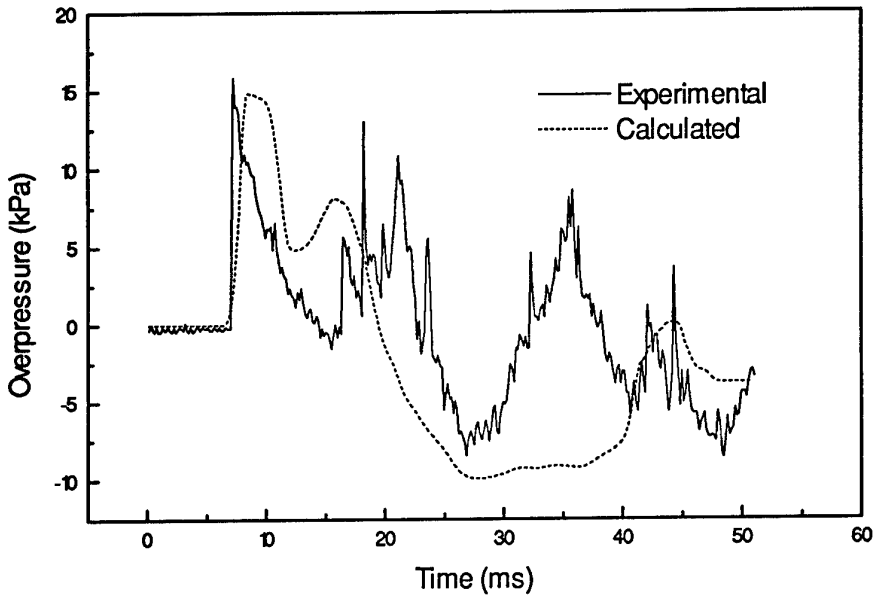

Figure 17. Plot of Overpressure versus Time for Gauge 4 in Event 10.

The contour plots for Event 10 are given in Figure 18a - 18k and are taken at a height of 0.7 m. The development of the shock wave expanding out from the explosion site (18b, 18c), reflecting off the concrete wall (18d, 18e, 18f), diffracting around the corner of the building (18c-18g) and inside the room in the building (18d-18i) can all be followed using these contour plots. The outstanding difference between event 3 and event 10 is the inclusion of the internal room in event 10 which is clearly shown in the contour plots.

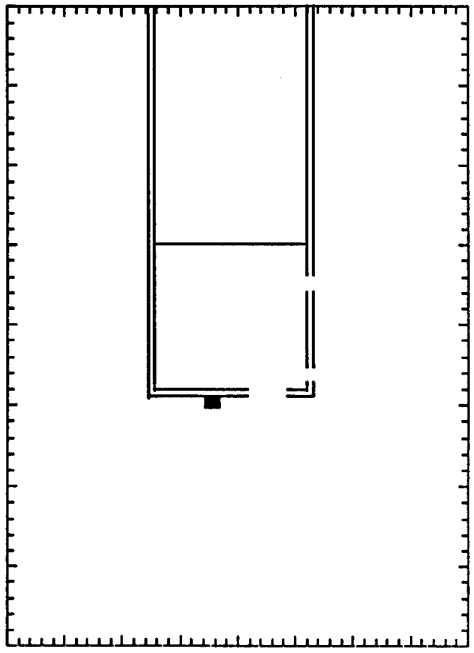

Figure 18a. 0.0ms contours with building outline superimposed

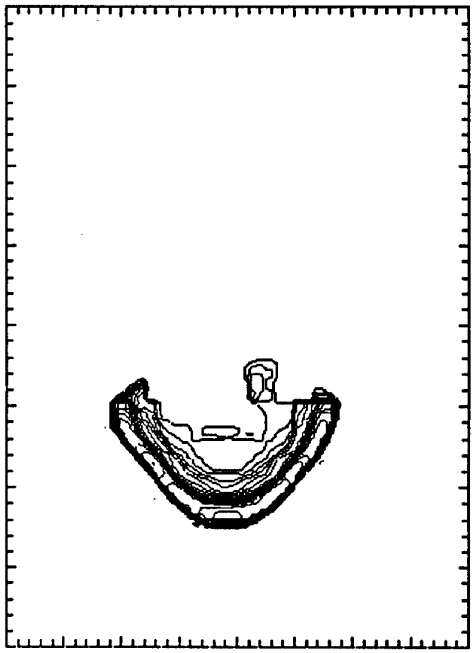

Figure 18b. 2.9ms contours

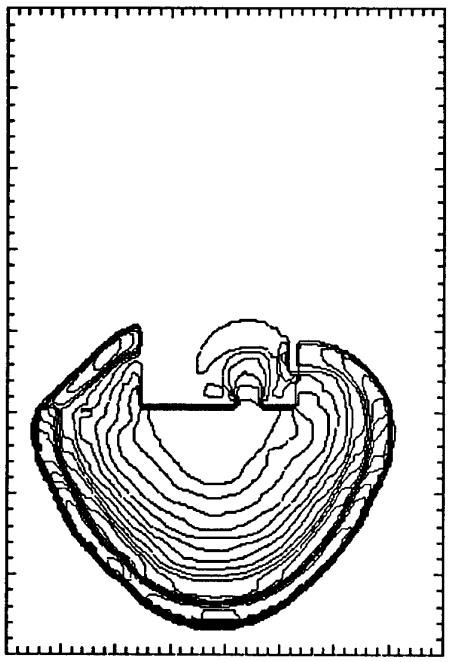

Figure 18c. 7.0ms contours

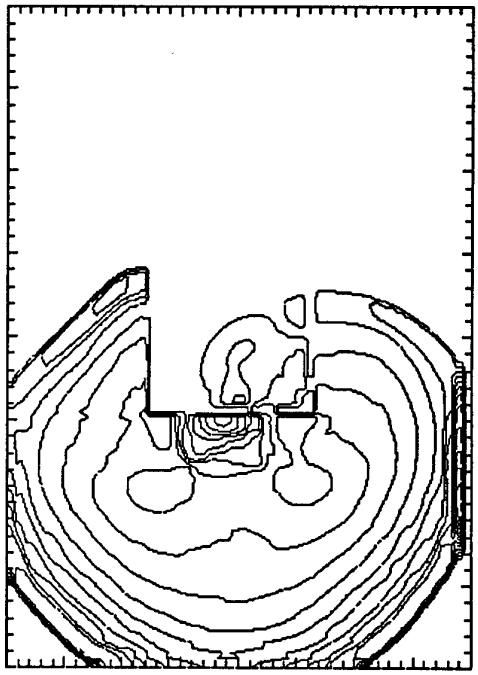

Figure 18d. 12.1ms contours

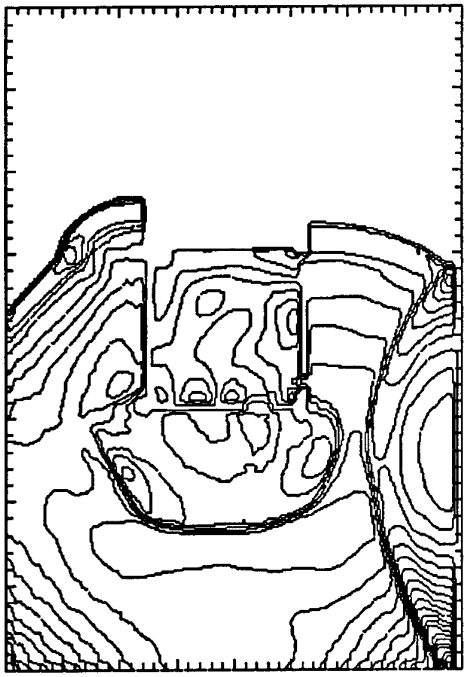

Figure 18e. 18.6ms contours

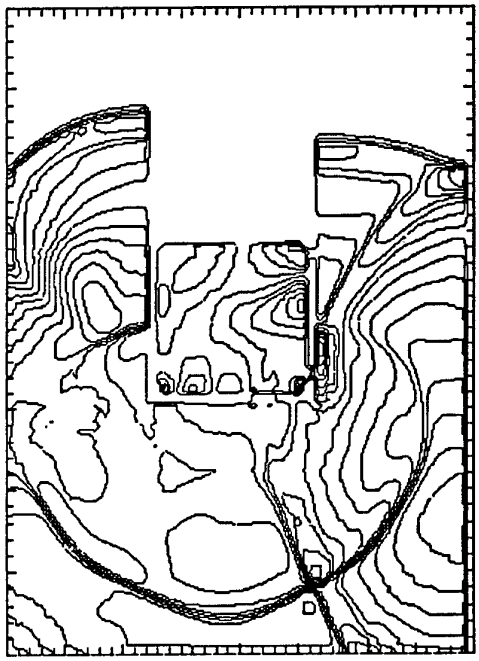

Figure 18f. 26.8ms contours

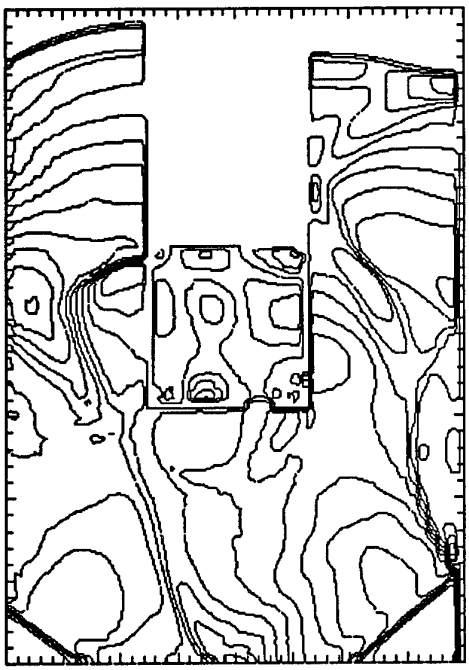

Figure 18g. 36.1ms contours

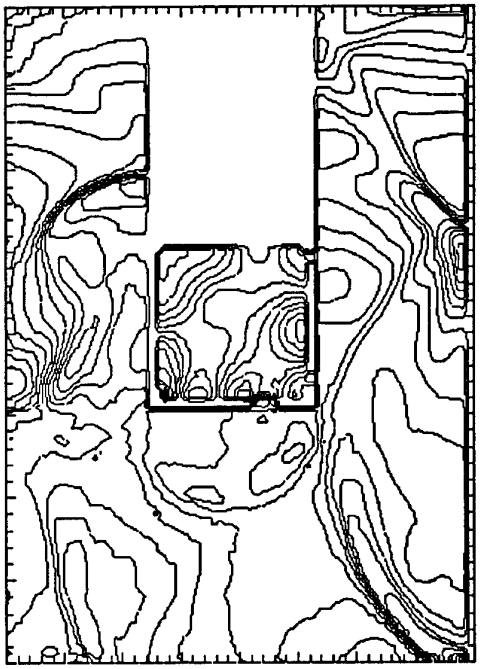

Figure 18h. 45.6ms contours

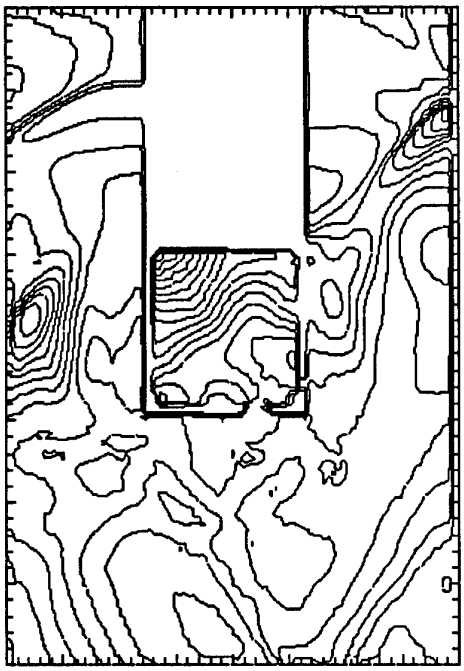

Figure 18i. 56.3ms contours

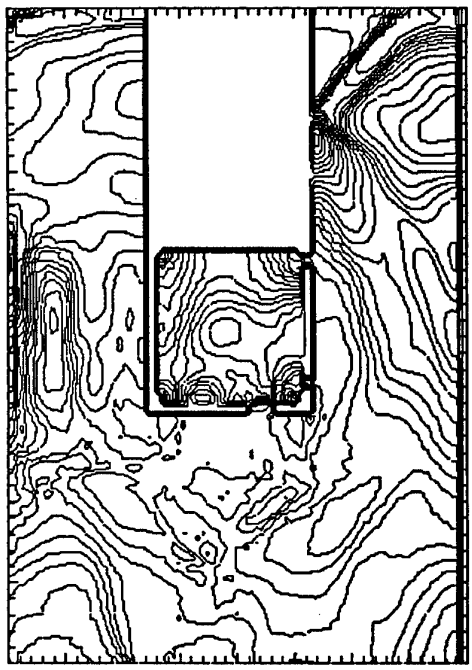

Figure 18j. 67.1ms contours

5. Conclusions

This paper represents the first successful modelling of the Australian Challenge in full 3-D geometry. The results in this paper have shown that the program has the ability to successfully calculate the blast overpressure from an explosion in a structurally complex scenario. This validation of the code will allow it to be used with confidence to model complex operational scenarios requiring the rapid entry of forces into buildings. It will reduce dramatically the need for expensive and time-consuming trials in this area and allow hypothetical situations to be explored. It will also allow the safety of current operational procedures to be evaluated, as well as any proposed changes to these procedures.

There are certain limitations on the capabilities of the code for doing these types of calculations given the size of the currently available computers. First, a computer memory size limitation means that a grid of approximately 1 million cells is the maximum that can be considered. This in turn directly limits the fineness of the grid that can be considered, for example, for a grid of 10 m x 10 m x 10 m the minimum cell size available is 10 cm x 10 cm x 10 cm. A less significant limitation is the duration of the calculation which is currently restricted to about 3000 timesteps. This allows the

calculation to be completed within about 1 week. This limitation precludes the use of the code in a real-time operational situation - the results will simply take too long to be of operational use.

A further limitation is that the program employs a Cartesian grid and consequently can only approximately represent non-Cartesian structures in the calculation. An example of this in the current calculations is the bent part of the 1.8 m high wall near the buildings. Since this part of the wall is at a non-90° angle it is represented by a stepwise construction rather than a smooth piece of wall. Similarly circular structures would not be well represented by the Cartesian grid because of the limitations imposed by the resolution of the calculation.

These limitations on the calculations do not present major restrictions on the use of the program but should be kept in mind when deciding whether this program will give the accuracy required in a desired situation. This work has shown that this program can successfully calculate the blast overpressure from an explosion in a large complex scenario of interest to the Australian Defence Forces. Consequently any similar problem, for example, the rapid entry of the Special Forces into buildings, will be able to be modelled with confidence and without resort to expensive field trials.

6. Acknowledgements

I acknowledge the efforts of P. Winter, L. Learmonth and D. Thornton in the design and conduct of the experimental test firings and G. Yiannakopoulos, A. Pleckauskas and F. Marian for the blast overpressure instrumentation at the test firings. I also wish to thank Phil Winter for his critical reading of this paper in the draft stages.

I am grateful to David Jones for his suggestion of the problem and for his useful advice during the work.

7. References

1. Memo to TTCP Demolitions Focus Officers from P. Winter regarding WTP-1 18th Annual Meeting, Action 41, June 28th, 1991.

2. Jones, David A., "Blast Overpressure Calculations for Wall-Breaching Charges", presented at TTCP TLG-3 Blast/Thermal Symposium, May 1992.

3. Combustion Dynamics, "Australian Challenge", internal report, July 1993.

4. Ohrt, Alan P., "Comparison of Predictions from the BlastinL Airblast Code to Data From the Woomera Demolitions Trial", presented at WTP - 18th Annual General Meeting.

5. BLAST3D code, written by Jones, David A. and Kemister, Gary.

6. Oran, Elaine S. and Boris, Jay P., "Numerical Simulation of Reactive Flow", Elsevier, New York, 1987.

This page intentionally left blank

Appendix 1:

Inclusion of an Arbitrary Geometry in the Program

The program is written in FORTRAN and so all of the programming examples used in this appendix use a FORTRAN style to illustrate the point.

The program has a 3-dimensional Cartesian grid as a basis for its computations. That is, when the program is integrating in each of the three directions it will loop over the number of points in each direction, e.g.,

```
      do 100 k=1,ncz
       do 110 j=1,ncy
        do 120 i=1,ncx
              .
              .
120      continue
110     continue
100   continue
```

In this case all the cells are being calculated since they are all included in the do-loop. To illustrate the way in which arbitrary geometries are included in three dimensions we will examine the 2-dimensional case. We then have the do-loops

```
      do 100 j=1,ncy
       do 110 i=1,ncx
              .
              .
110     continue
100   continue
```

and this can be represented graphically as

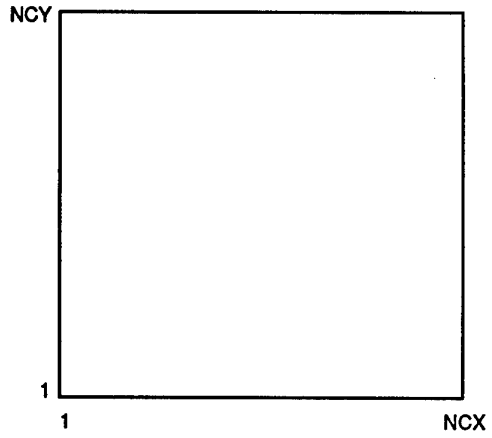

If we now want to exclude part of the area, e.g., between x=ncx/3 and x=2ncx/3 then we need to modify the do-loops to be

```
      do 100 j=1,ncy
       do 110 i=1,ncx/3
110    continue
       do 120 i=2ncx/3,ncx
            .
            .
120    continue
100   continue
```

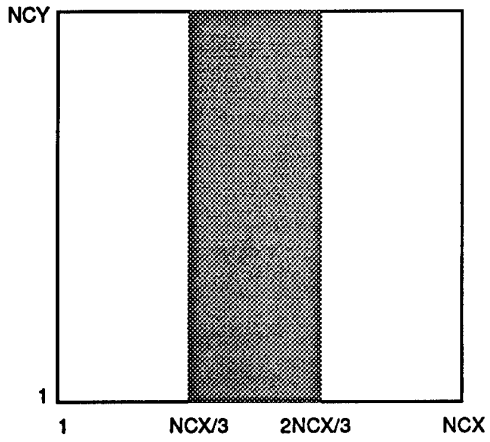

This approach can be generalised to an arbitrary number of excluded areas

```
      do 100 j=1,ncy
       do 110 iarea=1,inumarea
        ixmin=ileft(iarea)
        ixmax=iright(iarea)
        do 120 i=ixmin,ixmax
            .
            .
120     continue
110    continue
100   continue
```

where inumarea is the number of areas to be integrated, ixmin is the left limit for that area and ixmax is the right limit for that area. If further areas were to be excluded but which only extended part of the way along the y axis, e.g.,

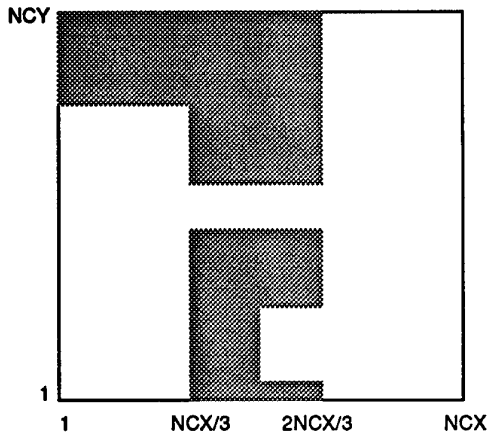

then this can be done in the following way

```
      do 100 j=1,ncy
       ixnumber=ixstep(j)
       do 110 istep=1,ixnumber
        ixmin=ileft(j,ixnumber)
        ixmax=iright(j,ixnumber)
        do 120 i=ixmin,ixmax
              .
              .
120      continue
110     continue
100    continue
```

where the array ixstep is the number of integrations for the value of j and the arrays ileft and iright are the left and right limits for each integration.

The next step is how to quickly and easily enter the limits of the integration represented in the arrays ileft and iright. The method chosen in this approach can be easily shown graphically below where the final geometry is simply built up by a series of overlaying levels which contain a rectangle, either solid to make an obstruction or empty to open up a space.

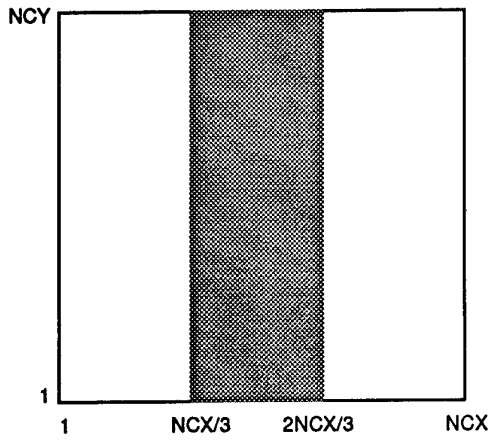

Addition of Solid1

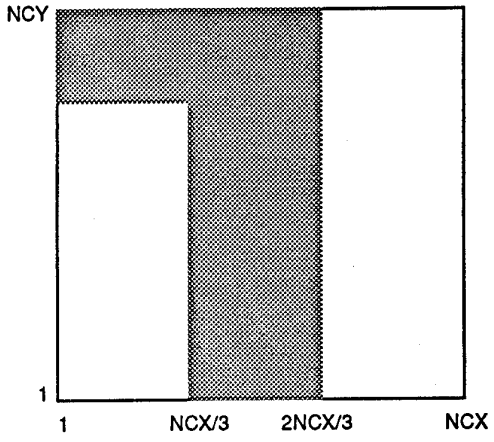

Addition of Solid2

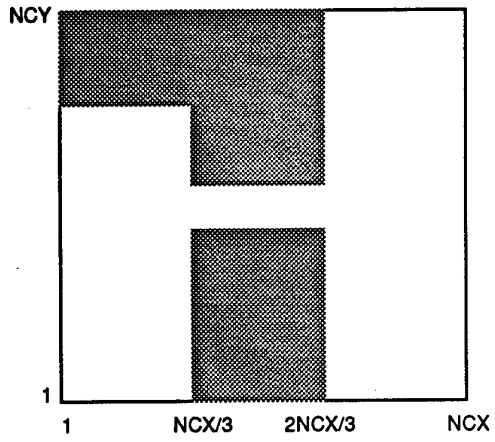

Addition of Open1

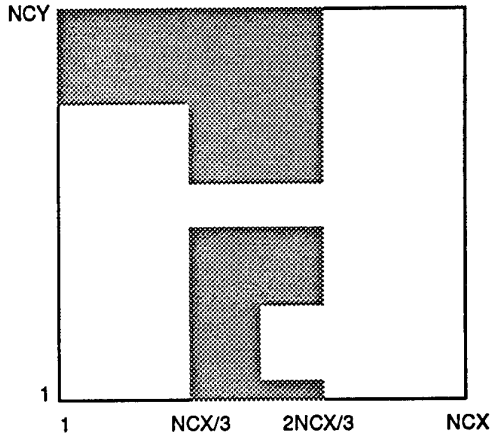

Addition of Open2

To take a more specific example, if we let ncx = ncy = 30 then we can specify the rectangles by their beginning and end points along each axis. For the solid rectangles we have the coordinates

	xmin	xmax	ymin	ymax
solid1	10	20	1	30
solid2	1	10	22	30

and for the open rectangles we have the coordinates

	xmin	xmax	ymin	ymax
open1	10	20	14	17
open2	15	20	2	8

where solid1 has the corners (proceeding clockwise from the lower left) (10,1),(10,30),(20,30),(20,1).

The question remains of how do we translate these numbers to obtain the correct limits for the integrations. Again this can best be shown by example. We shall examine several specific points along the y axis, namely, y=10, y=28, y=15 and y=5 which will show the addition of each rectangle (these lines are shown in the figure below)

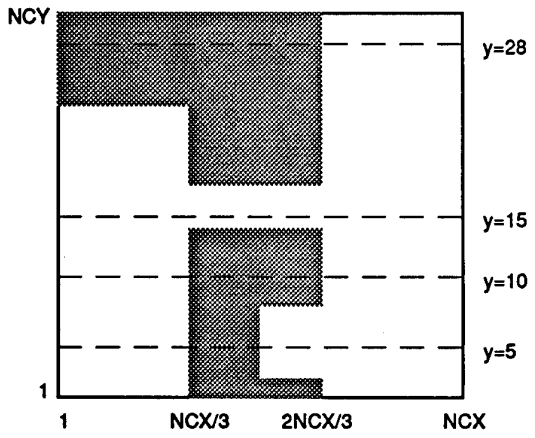

For y=10 the integration limits after each addition are

		left	right
initial		1	30
additions	solid1	1	10
		20	30
	solid2	1	10
		20	30
	open1	1	10
		20	30
	open 2	1	10
		20	30
final		1	10
		20	30

For y=28 the integration limits after each addition are

		left	right
initial		1	30
additions	solid1	1	10
		20	30
	solid2	20	30
	open1	20	30
	open 2	20	30
final		20	30

For y=15 the integration limits after each addition are

		left	right
initial		1	30
additions	solid1	1	10
		20	30
	solid2	1	10
		20	30
	open1	1	30
	open 2	1	30
final		1	30

For y=10 the integration limits after each addition are

		left	right
initial		1	30
additions	solid1	1	10
		20	30
	solid2	1	10
		20	30
	open1	1	10
		20	30
	open 2	1	10
		15	30
final		1	10
		15	30

That is the limits for a particular y value change whenever the rectangle includes that value. In this way we can build up quite complex shapes by adding either solid or open rectangles and consequently adjusting the limits of integration for each addition.

These concepts and procedures are quite easily extended to three dimensions by adding a further do-loop, e.g.,

```
      do 100 k=1,ncz
       do 110 j=1,ncy
        ixnumber=ixstep(j,k)
        do 120 istep=1,ixnumber
         ixmin=ileft(j,k,ixnumber)
         ixmax=iright(j,k,ixnumber)
         do 130 i=ixmin,ixmax
              .
              .
130       continue
120      continue
110     continue
100   continue
```

Computational Fluid Dynamics Modelling of the Australian Challenge

G. Kemister

DSTO-TR-0224

DISTRIBUTION LIST

AUSTRALIA

DEFENCE ORGANISATION

Defence Science and Technology Organisation

Chief Defence Scientist
FAS Science Policy
AS Science Corporate Management
} shared copy

Counsellor Defence Science, London (Doc Data Sheet only)
Counsellor Defence Science, Washington (Doc Data Sheet only)
Scientific Adviser to Thailand MRD (Doc Data Sheet only)
Scientific Adviser to the DRC (Kuala Lumpur) (Doc Data Sheet only)
Senior Defence Scientific Adviser/Scientific Adviser Policy and Command shared copy
Navy Scientific Adviser (3 copies Doc Data Sheet only)
Scientific Adviser - Army (Doc Data Sheet only)
Air Force Scientific Adviser
Director Trials

Originating Laboratory

Director (AMRL only)
Chief Weapons Systems Division
Dr R.J. Spear, RLLWS, WSD
Dr D.A. Jones, WSD
Dr R.A.J. Borg, WSD
Dr N. Burman, SSMD
Author: Dr G. Kemister, WSD

DSTO Library

Library Fishermens Bend
Library Maribyrnong
Main Library DSTOS (2 copies)
Library, MOD, Pyrmont (Doc Data sheet only)

Defence Central

OIC TRS, Defence Central Library
Officer in Charge, Document Exchange Centre, 12 copies
Defence Intelligence Organisation
Library, Defence Signals Directorate (Doc Data Sheet only)

Army

Director General Force Development (Land), (Doc Data Sheet only)
ABCA Office, G-1-34, Russell Offices, Canberra (4 copies)
NAPOC QWG Engineer NBCD c/- DENGRS-A, HQ Engineer Centre

Navy

ASSTASS, APW2-1-OA2, Anzac Park West, Canberra, (Doc Data Sheet only)

Dr Paul Thibbault, Combustion Dynamics Ltd, Canada
Special Forces, Swanbourne, WA
HQSF, Russell Offices, Canberra
Engineers, SME, Moorebank
DGFD (Sea)
DGFD (Air)
FDA-ASU
DLPD-AF Attn. WGCDR D. Tramoundanis
DNW
DGMAT-A

UNIVERSITIES AND COLLEGES

Australian Defence Force Academy
Library
Head of Aerospace and Mechanical Engineering
Deakin University, Serials Section (M list)), Deakin University Library, Geelong, 3217,
Senior Librarian, Hargrave Library, Monash University

OTHER ORGANISATIONS

NASA (Canberra) (Doc Data Sheet only)
AGPS

ABSTRACTING AND INFORMATION ORGANISATIONS

INSPEC: Acquisitions Section Institution of Electrical Engineers
Library, Chemical Abstracts Reference Service
Engineering Societies Library, US
American Society for Metals
Documents Librarian, The Center for Research Libraries, US

INFORMATION EXCHANGE AGREEMENT PARTNERS

Acquisitions Unit, Science Reference and Information Service, UK
Library - Exchange Desk, National Institute of Standards and Technology, US

SPARES (40 copies)

TOTAL (96 copies)

DEFENCE SCIENCE AND TECHNOLOGY ORGANISATION DOCUMENT CONTROL DATA	1. PAGE CLASSIFICATION UNCLASSIFIED 2. PRIVACY MARKING/CAVEAT (OF DOCUMENT)

3. TITLE	4. SECURITY CLASSIFICATION (FOR UNCLASSIFIED REPORTS THAT ARE LIMITED RELEASE USE (L) NEXT TO DOCUMENT CLASSIFICATION)
Computational fluid dynamics modelling of the Australian Challenge	Document (U) Title (U) Abstract (U)
5. AUTHOR(S) G. Kemister	6. CORPORATE AUTHOR Aeronautical and Maritime Research Laboratory PO Box 4331 Melbourne Vic 3001

7a. DSTO NUMBER	7b. AR NUMBER	7c. TYPE OF REPORT	8. DOCUMENT DATE
DSTO-TR-0224	AR-009-356	Technical Report	September 1995

9. FILE NUMBER	10. TASK NUMBER	11. TASK SPONSOR	12. NO. OF PAGES	13. NO. OF REFERENCES
510/207/0243	DST 93/103	DSTO	41	6

14. DOWNGRADING/DELIMITING INSTRUCTIONS	15. RELEASE AUTHORITY
Not applicable	Chief Weapons Systems Division

16. SECONDARY RELEASE STATEMENT OF THIS DOCUMENT

Approved for public release

OVERSEAS ENQUIRIES OUTSIDE STATED LIMITATIONS SHOULD BE REFERRED THROUGH DOCUMENT EXCHANGE CENTRE, DIS NETWORK OFFICE, DEPT OF DEFENCE, CAMPBELL PARK OFFICES, CANBERRA ACT 2600

17. DELIBERATE ANNOUNCEMENT

Announcement of this report is unlimited

18. CASUAL ANNOUNCEMENT YES

19. DEFTEST DESCRIPTORS

Explosion effects	RDX	Shelters
Over pressure	Computerized simulation	
Explosives	Buildings	

20. ABSTRACT

The Australian Challenge was a set of experiments chosen as a test case to establish how well computer calculations can model the blast overpressure around a complex set of structures. This paper presents the first three dimensional calculation on the Australian Challenge using CFD codes. These codes have been developed at AMRL and the Australian Challenge represents their first test in a 'real world' scenario. The calculations show good agreement with the experimental results. The program can now be used with a good degree of confidence in modelling other complex scenarios, reducing the need for expensive experimentation. The safety aspects of any changes in operational procedure can be evaluated quickly and efficiently.